Combining baffles and secondary porous layers for performance enhancement of proton exchange membrane fuel cells (Supplementary Materials)

Luka Mihanović[1], Željko Penga[2,3*], Lei Xing[4,5*], Viktor Hacker[6]

[1] *Croatian Defense Academy, University of Split, Naval studies, Split, Croatia*

[2]*Faculty of electrical engineering, mechanical engineering and naval architecture, University of Split, Split, Croatia*

[3]*Center for Excellence for Science and Technology – Integration of Mediterranean Region, University of Split, Split, Croatia*

[4]*Department of Engineering Science, University of Oxford, Oxford, UK*

[5]*Institute of Green Chemistry and Chemical Technology, Jiangsu University, Zhenjiang, China*

[6] *Institute of Chemical Engineering and Environmental Technology, Graz University of Technology, Graz, Austria*

**Corresponding author emails:*

zpenga@fesb.hr (Željko Penga)

xinglei1314@gmail.com; xinglei@ujs.edu.cn (Lei Xing)

1. Model development

1.1.1. Electrochemistry

Two potential equations are solved. One accounts for the electron transport through the solid materials resolved in the triple-phase boundaries (TPBs) of the CL, solid component of the GDL, and collectors. The second equation resolves the ionic transport of protons inside the TPBs and the polymer electrolyte membrane. The equations are written as:

$$\nabla \cdot (\sigma_{sol} \nabla \phi_{sol}) + R_{sol} = 0 \quad (1)$$

$$\nabla \cdot (\sigma_{mem} \nabla \phi_{mem}) + R_{mem} = 0 \quad (2)$$

where σ represents electrical conductivity, ϕ electric potential and R volumetric transfer current. Zero flux for ϕ_{mem} is prescribed on all outside walls. There are external boundaries for the solid phase potential ϕ_{sol} at the anode and cathode side, representing the external electric circuit and the current generated by the cell passes through the specified boundaries, i. e. current collectors. On the remaining external walls ϕ_{sol} is set to zero flux. ϕ_{sol} on the cathode side can be set to constant flux or constant value, representing galvanostatic or potentiostatic boundary conditions, respectively. The transfer current source terms, specified in Eqns. (1) and (2), are non-zero only in the CLs, computed as follows.

For the potential equation in solid phase:

$$R_{sol} = -R_{an} (< 0) \quad (3)$$

$$R_{sol} = +R_{cat} (> 0) \quad (4)$$

For the potential equation in the electrolyte phase:

$$R_{mem} = +R_{an} (> 0) \quad (5)$$

$$R_{mem} = -R_{cat} (< 0) \quad (6)$$

where the subscripts an (in Eqns. 3 and 5) and cat (in Eqns. 4 and 6) present the anode and cathode, respectively. The source terms in Eqns. (3)-(6) represent the exchange current density, defined as:

$$R_{an} = \left(\zeta_{an} j_{an}(T)\right)\left(\frac{[A]}{[A]_{ref}}\right)^{\gamma_{an}}\left(e^{\frac{\alpha_{an}^{an} F \eta_{an}}{RT}} + e^{-\frac{\alpha_{cat}^{an} F \eta_{an}}{RT}}\right) \tag{7}$$

$$R_{cat} = \left(\zeta_{cat} j_{cat}(T)\right)\left(\frac{[C]}{[C]_{ref}}\right)^{\gamma_{cat}}\left(-e^{\frac{\alpha_{an}^{cat} F \eta_{cat}}{RT}} + e^{-\frac{\alpha_{cat}^{cat} F \eta_{cat}}{RT}}\right) \tag{8}$$

where $j(T)$ represents reference exchange current density per active surface area, ζ specific active surface area, γ concentration dependence, α_{an}^{an} and α_{cat}^{an} anode and cathode transfer coefficients on the anode electrode, respectively, α_{an}^{cat} and α_{cat}^{cat} anode and cathode transfer coefficients on the cathode electrode, respectively, η_{an} surface overpotential on the anode, η_{cat} surface overpotential on the cathode, F Faraday constant, R universal gas constant, T temperature, $[A]$ and $[C]$ molar concentration of species, where A represents H_2 and C represents O_2. The subscript ref represents reference concentration. When the surface over-potential is large, the Butler-Volmer formulation (Eqns. 7 and 8) reduces to Tafel formulation as follows:

$$R_{an} = \zeta_{an} j_{an}(T)\left(\frac{[A]}{[A]_{ref}}\right)^{\gamma_{an}}\left(e^{\frac{\alpha_{an} F \eta_{an}}{RT}}\right) \tag{9}$$

$$R_{cat} = \zeta_{cat} j_{cat}(T)\left(\frac{[C]}{[C]_{ref}}\right)^{\gamma_{cat}}\left(e^{\frac{\alpha_{cat} F \eta_{cat}}{RT}}\right) \tag{10}$$

Reference exchange current density formulation is temperature dependent as follows:

$$j_{an}(T) = j_{an}^{ref} e^{-\frac{E_{an}}{RT\left(1-\frac{T}{T_{an}^{ref}}\right)}} \tag{11}$$

$$j_{cat}(T) = j_{cat}^{ref} e^{-\frac{E_{cat}}{RT\left(1-\frac{T}{T_{cat}^{ref}}\right)}} \tag{12}$$

where E represents user-specified activation energy, T_{an}^{ref} and T_{cat}^{ref} user-specified reference temperature and j_{an}^{ref} and j_{cat}^{ref} reference exchange current density specified at the reference temperature.

Activation loss is specified as:

$$\eta_{an} = \phi_{sol} - \phi_{mem} - U_{an}^{0} \tag{13}$$

$$\eta_{cat} = \phi_{sol} - \phi_{mem} - U_{cat}^{0} \tag{14}$$

The anode and cathode half-cell potentials are computed according to the Nernst equations:

$$U_{an}^{0} = E_{an}^{0} - \frac{\Delta S_{an}}{2F}(T - T_0) - \frac{RT}{2F}\ln(\frac{p_{H_2}}{p^0}) \tag{15}$$

$$U_{cat}^{0} = E_{cat}^{0} + \frac{\Delta S_{cat}}{2F}(T - T_0) - \frac{RT}{2F}\ln\left(\frac{p_{H_2O}}{p_{sat}\sqrt{\frac{p_{O_2}}{p^0}}}\right) \tag{16}$$

where p_{sat} represents water saturation pressure, p_{H_2}, p_{O_2}, and p_{H_2O} partial pressures of hydrogen, oxygen and water vapor, respectively. Standard state variables T^0 and p^0, reversible potentials E_{an}^{0} and E_{cat}^{0}, and reaction entropies ΔS_{an} and ΔS_{cat} are user-specified. Two potential fields are obtained by solving Eqns. (1) - (16).

1.1.2. Cathode particle model

The mass transport resistance within the porous electrode is not considered in the B-V equations, i. e. Eqns. (9) and (10) [27]. Otherwise, the calculated resistance consists of two parts: the resistance of the ionomer film, $\Re_{ion}$, and resistance due to liquid water film surrounding the catalyst particles, $\Re_{liq}$. The volumetric transfer current inside the cathode CL is expressed as:

$$R_{cat} = 4F\frac{c_{O_2}}{\frac{c_{O_2}}{j_{O_2}^{ideal}} + \Re_{ion} + \Re_{liq}} \tag{17}$$

where c_{O_2} is concentration of O_2 at the wall, $\Re_{ion}$ is user-specified, $\Re_{liq}$ is calculated as:

$$\Re_{liq} = \frac{\zeta_{cat} r_p^2}{K_w D_w} \cdot \frac{\sqrt[3]{1 + \frac{S\varepsilon}{1-\varepsilon}}}{3(1-\varepsilon)} \tag{18}$$

where ζ_{cat} represents active surface area of the cathode catalyst layer, s liquid saturation, ε porosity, r_p particle diameter and $K_w D_w$ product of oxygen solubility in liquid water, while $j_{O_2}^{ideal}$ is calculated as:

$$j_{O_2}^{ideal} = \frac{R_{cat}^0}{4F} \tag{19}$$

where R_{cat}^0 represents ideal transfer current computed according to Eq. (8) without considering the resistance.

1.1.3. Conservation of current and mass

Source terms for H_2, O_2 and dissolved water content λ in the CLs due to electrochemical reactions have the following form:

$$S_{H_2} = -\frac{M_{w,H_2}}{2F} R_{an} < 0 \tag{20}$$

$$S_{O_2} = -\frac{M_{w,O_2}}{4F} R_{cat} < 0 \tag{21}$$

$$S_{\lambda} = -\frac{M_{w,H_2O}}{2F} R_{cat} > 0 \tag{22}$$

where M_{w,H_2}, M_{w,O_2} and M_{w,H_2O} represent molecular masses of the species, F Faraday constant, as previously mentioned, and 2 and 4 the number of electrons per mole of the reactants and products.

The conservation is achieved by equal production of the current at the anode and cathode catalyst layer, and is written as follows:

$$\int_{an} R_{an} dV = \int_{cat} R_{cat} dV \tag{23}$$

1.1.4. Water transport and mass transfer

Water inside the PEM fuel cell exists in three phases: dissolved, liquid, and gaseous, i. e. water vapour. The dissolved phase exists in the membrane/ionomer phase of the CLs and inside the membrane, while the generation and transport of dissolved water is described by the following expression in [28].

$$\frac{\partial}{\partial t}\left(\frac{\varepsilon_i M_{w,H_2O}\rho_i\lambda}{EW}\right)+\nabla\cdot\left(\frac{\vec{\imath}_m n_d M_{w,H_2O}}{F}\right) = \nabla\cdot\left(M_{w,H_2O}D_w^i\nabla\lambda\right)+S_\lambda+S_{gd}+S_{ld} \tag{24}$$

where ε_i represents porosity of the porous media, $\vec{\imath}_m$ ionic current density (with $\vec{\imath}_m = -\sigma_{mem}\nabla\phi_{mem}$), λ dissolved water content, n_d osmotic drag coefficient, D_w^i diffusion coefficient of water content, S_λ water generation in the cathode catalyst layer due to electrochemical reaction, S_{gd} mass change between the gaseous and dissolved phase and S_{ld} mass change between the liquid and dissolved phase, calculated as [27].

$$S_{gd} = \left(1-s^\theta\right)\gamma_{gd}M_{w,H_2O}\frac{\rho_i}{EW}(\lambda_{eq}-\lambda) \tag{25}$$

$$S_{ld} = s^\theta\gamma_{ld}M_{w,H_2O}\frac{\rho_i}{EW}(\lambda_{eq}-\lambda) \tag{26}$$

where ρ_i represents dry ionomer, or membrane, density, EW equivalent weight of the membrane, s liquid saturation, λ_{eq} equilibrium water content, γ_{gd} and γ_{ld} gas and liquid mass exchange rate constants, while γ_{gd}, γ_{ld} and θ are user-specified constants.

Equilibrium water content is expressed as [27]:

$$\lambda_{eq} = 0.36+6a(1-\tanh(a-0.5)) + 0.69(\lambda_{a=1}-3.52)a^{0.5}\left(1+\tanh\left(\frac{a-0.89}{0.23}\right)\right)+s(\lambda_{s=1} \tag{27}$$

where a represents water activity, defined as:

$$a = \frac{p_{wv}}{p_{sat}} \tag{28}$$

where p_{wv} represents water vapor partial pressure and p_{sat} water vapor saturation pressure, while $\lambda_{s=1}$ and $\lambda_{a=1}$ are user-specified parameters which can be used to fit the function according the experimental measurement data, e.g. Zawodzinski et al. [29], Hinatsu et al. [30], or custom membrane water content equations. In this work, the data is fitted to represent the original Zawodzinski's expression which resulted in the most accurate prediction as seen in previous studies [31,32].

Liquid water is considered in all porous electrodes and gas channels. The driving force for liquid water transport is the liquid pressure gradient ∇p_l, calculated as

$$\frac{\partial}{\partial t}(\varepsilon_i \rho_l s) = \nabla \cdot \left(\frac{\rho_l K K_r}{\mu_l} \nabla p_l\right) + S_{gl} - S_{ld} \tag{29}$$

where ρ_l represents liquid water density, μ_l absolute viscosity, K absolute permeability, K_r relative permeability, p_l liquid pressure and S_{gl} and S_{ld} mass change between gas and liquid phase, and liquid and dissolved phase, respectively. K_r In GDLs and MPLs is computed as:

$$K_r = s^b \tag{30}$$

where s represents liquid saturation and b is user-defined constant. In the membrane K_r is computed as:

$$K_r = \left(\frac{\frac{M_{w,H_2O}}{\rho_l}\lambda_{S=1} + \frac{EW}{\rho_i}}{\frac{M_{w,H_2O}}{\rho_l}\lambda + \frac{EW}{\rho_i}} \cdot \frac{\lambda}{\lambda_{s=1}}\right)^2 \tag{31}$$

Substituting p_l from Eq. (29) with the sum of capillary pressure p_c and gas pressure p, Eq. (29) is redefined to:

$$\frac{\partial}{\partial t}(\varepsilon_i \rho_l s) = \nabla \cdot \left(\frac{\rho_l K K_r}{\mu_l} \nabla (p_c + p)\right) + S_{gl} - S_{ld} \tag{32}$$

while the mass transfer rate between the liquid and gas phases is computed based on the unidirectional diffusion expressions as follows. When $p_{wv} \leq p_{sat}$, we have:

$$S_{gl} = \frac{\gamma_e \varepsilon s D_{gl} M_{w,H_2O}}{RT} p ln\left(\frac{p - p_{sat}}{p - p_{wv}}\right) \tag{33}$$

otherwise,

$$S_{gl} = \frac{\gamma_c \varepsilon (1 - s) D_{gl} M_{w,H_2O}}{RT} p ln\left(\frac{p - p_{sat}}{p - p_{wv}}\right) \tag{34}$$

where ε represents porosity, γ_e evaporation and γ_c condensation rate coefficient, and D_{gl} is calculated as follow. At the cathode side:

$$D_{gl} = 0.365 \cdot 10^{-4} \left(\frac{T}{343}\right)^{2.334} \cdot \left(\frac{10^5}{p}\right) \tag{35}$$

At the anode side:

$$D_{gl} = 1.79 \cdot 10^{-4} \left(\frac{T}{343}\right)^{2.334} \cdot \left(\frac{10^5}{p}\right) \tag{36}$$

Eq. (32) is solved in all regions between the anode and cathode GDL-channel interfaces. At the specified interfaces, the water flux is only allowed in the gas channel direction, without the possibility for back-flow, and the water flux is driven by the capillary pressure as follows:

$$f_{liq} = \Theta\varepsilon\, \mathrm{s} \cdot \max\left[\left(p_c + \frac{1}{2}\rho v^2\right), 0\right] \tag{37}$$

where θ represents coefficient of liquid water removal. Liquid saturation is computed using Leverett function. For hydrophilic materials withcontact angle $\theta_c < 90°$, the capillary pressure is expressed as:

$$p_c = \sigma cos\theta_c \sqrt{\frac{\varepsilon}{K}} J(1-s) \tag{38}$$

where σ is surface tension, and for hydrophobic materials withcontact angle $\theta_c > 90°$, we have:

$$p_c = \sigma cos\theta_c \sqrt{\frac{\varepsilon}{K}} J(s) \tag{39}$$

The Leverett function can be expressed as the following polynomial expression:

$$J(x) = \mathrm{a}x - \mathrm{b}x^2 + \mathrm{c}x^3 \tag{40}$$

where a, b, and c are user-specified Leverett function coefficients (standard value 1.417, 2.12 and 1.263, respectively). The reduction of the effective surface area of the catalyst is modeled by modifying the transfer current by adopting the following expression:

$$R_j = (1-s)^{\gamma_j} R_j \tag{41}$$

where γ_j is user-specified parameter.

Liquid water transport inside the channels is tracked using the correlation as follow:

$$\frac{\partial}{\partial t}(\rho_l s) + \nabla \cdot (\rho_l \vec{v}_l s) = \nabla \cdot (D_{liq} \nabla s) \tag{42}$$

where D_{liq} represents liquid water diffusion coefficient in the channels and $\vec{v}_l$ liquid velocity being a fraction of the gas velocity $\vec{v}_g$

$$\vec{v}_l = \chi \vec{v}_g \tag{43}$$

where χ represents liquid to gas velocity ratio. The phase-change in the channels is not considered, since it is assumed that the flow is convection-dominated.

1.1.5. Heat sources

Volumetric heat sources are calculated according to the following expressions. Inside the GDL and MPL ($S_{GDL+MPL}$), anode CL (S_{ACL}), cathode CL (S_{CCL}), membrane (S_{MEM}), and current collector solid (S_{CC}), the heat source is respectively described by the following expressions as:

$$S_{GDL+MPL} = \frac{i_s^2}{\sigma_{sol}} - S_{gl^*} \cdot L \tag{44}$$

$$S_{ACL} = R_{an}\left(\eta_{an} - \frac{T\Delta S_{an}}{2F}\right) + \frac{i_s^2}{\sigma_{sol}} + \frac{i_m^2}{\sigma_{mem}} - \left(S_{dl} + S_{gl}\right) \cdot L \tag{45}$$

$$S_{CCL} = R_{cat}\left(-\eta_{cat} - \frac{T\Delta S_{cat}}{2F}\right) + \frac{i_s^2}{\sigma_{sol}} + \frac{i_m^2}{\sigma_{mem}} - \left(S_{dl} + S_{gl}\right) \cdot L \tag{46}$$

$$S_{MEM} = \frac{i_m^2}{\sigma_{mem}} \tag{47}$$

$$S_{CC} = \frac{i_s^2}{\sigma_{sol}} \tag{48}$$

where i_s and i_m represent the current densities of solid and electrolyte phase, respectively, and $L < 0$ latent heat of condensation. Heat sources in the gas channels are not modeled.

1.1.6. Material properties

Gas species diffusivity is computed using dilute approximation or full multi-component diffusion. The dilute approximation is calculated as:

$$D_i = \varepsilon^{1.5}(1-s)^{r_s} D_i^0 \left(\frac{p_0}{p}\right)^{\gamma_p} \left(\frac{T}{T_0}\right)^{\gamma_t} \tag{49}$$

where ε represents the porosity of the porous media, D_i^0 mass diffusivity of the species i at reference pressure ($p_0 = 101325\, Pa$) and temperature ($T_0 = 300\, K$). The reference values for the exponents are $\gamma_p = 1.0$, $\gamma_t = 1.5$, pore blockage exponent $r_s = 2.5$. Full multicomponent diffusion with tortuosity correction is calculated according to the following expression [26]:

$$D_{eff}^{ij} = (1-s)^{r_s} \varepsilon^{1.5} D^{ij} \tag{50}$$

where D_{eff}^{ij} represents the effective diffusivity, while the D^{ij} is the diffusivity calculated by the full multicomponent diffusion method, as described in more detail in the software manual [26].

Electrolyte phase ionic conductivity is calculated based on the following expression:

$$\sigma_{mem} = \Gamma_i (0.514\lambda - 0.326)^{\omega_i} e^{E_i\left(\frac{1}{303}+\frac{1}{T}\right)} \tag{51}$$

where λ represents membrane/ionomer water content, E_i activation energy for the temperature correction term, and Γ_i of the membrane, the ionomer in the anode and cathode CLs are calculated respectively according to the following expression:

$$\Gamma_i = \beta_{mem} \tag{52}$$

$$\Gamma_i = \beta_{an}^{\frac{\varsigma_a}{\tau_a}} \tag{53}$$

$$\Gamma_i = \beta_{cat}^{\frac{\varsigma_c}{\tau_c}} \tag{54}$$

where ς_a and ς_c represents the anode and cathode ionomer volume fraction and τ_a and τ_c anode and cathode CLs tortuosity, respectively. Parameters β and ω are introduced for generality purpose.

The diffusivity coefficient of dissolved water transport through membrane and ionomer is calculated as:

$$D_w^i = \frac{\eta_\lambda \rho_i}{EW} f(\lambda) \tag{55}$$

where η_λ represents user-defined generality coefficient, while $f(\lambda)$ for is given as follow according to Wu et al. [28] or according to Wang and Wang [33], who adopted it from Motupally et al. [34] who presented it first. In this work, Wu [28] model was considered.

$$f(\lambda) = 4.1 \cdot 10^{-10} \left(\frac{\lambda}{25}\right)^{0.15} \left[1 + \tanh\left(\frac{\lambda - 2.5}{1.4}\right)\right] \tag{56}$$

The osmotic drag coefficient n_d is calculated as:

$$n_d = n_{osm} g(\lambda) \tag{57}$$

where η_{osm} is user-defined generality coefficient, set in this work to the default value of 1.0, according to the referenced suggestions [34], and the function $g(\lambda)$ represents standard Springer et al. [35] expression as:

$$g(\lambda) = \frac{2.5\lambda}{22} \tag{58}$$

The saturation pressure, converted to archaic units atm is calculated according to the expression of

$$\log_{10} p_{sat} = a + bt + ct^2 + dt^3 \tag{59}$$

where t represents temperature in $°C$, and saturation coefficients are equal to $a = -2.1794$, $b = 0.02953$, $c = -9.1837\times10^{-5}$ and $d = 1.4454\times10^{-7}$.

1.1.7. Cross-over current

The cross-over current, is accounted by introducing the following source terms:

$$S_{H_2} = -\frac{M_{w,H_2}}{2F} \cdot \frac{I_l}{Vol_{an}} \tag{60}$$

$$S_{O_2} = -\frac{M_{w,O_2}}{4F} \cdot \frac{I_l}{Vol_{cat}} \tag{61}$$

$$S_\lambda = \frac{M_{w,H_2O}}{2F} \cdot \frac{I_l}{Vol_{cat}} \tag{62}$$

where Vol_{an} and Vol_{cat} represent the anode and cathode CL volumes, respectively, and numbers 2 and 4 are number of electrons per mole of reactants and products,the volumetric cross-over current I_l/Vol_{cat} is subtracted from the cathode transfer current R_{cat} in Eqns. (8) or (10), accordingly.

2. Results and discussion

Flow regimes in porous media are shown in Figure S1. Area marked with 1 is dominated by Darcy's law, 2 by weak inertial forces, 3 with Forchheimer's regime, i.e. intense inertia, 4 is transition between Forchheimer's and turbulent regime, and 5 it turbulent regime.

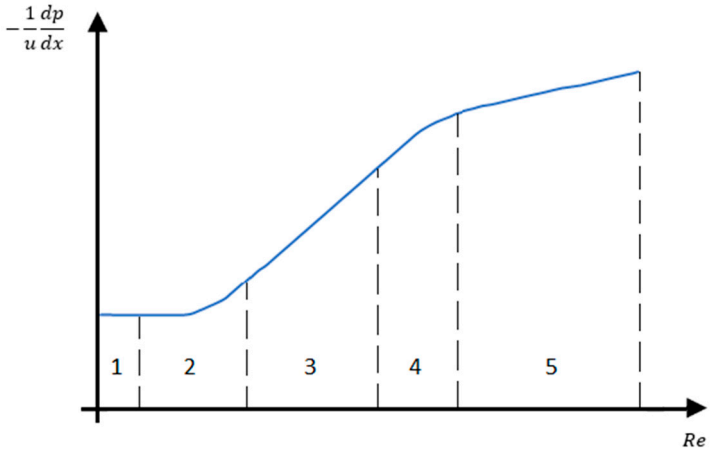

Figure S1. Flow regimes in porous media, Takhanov [36].

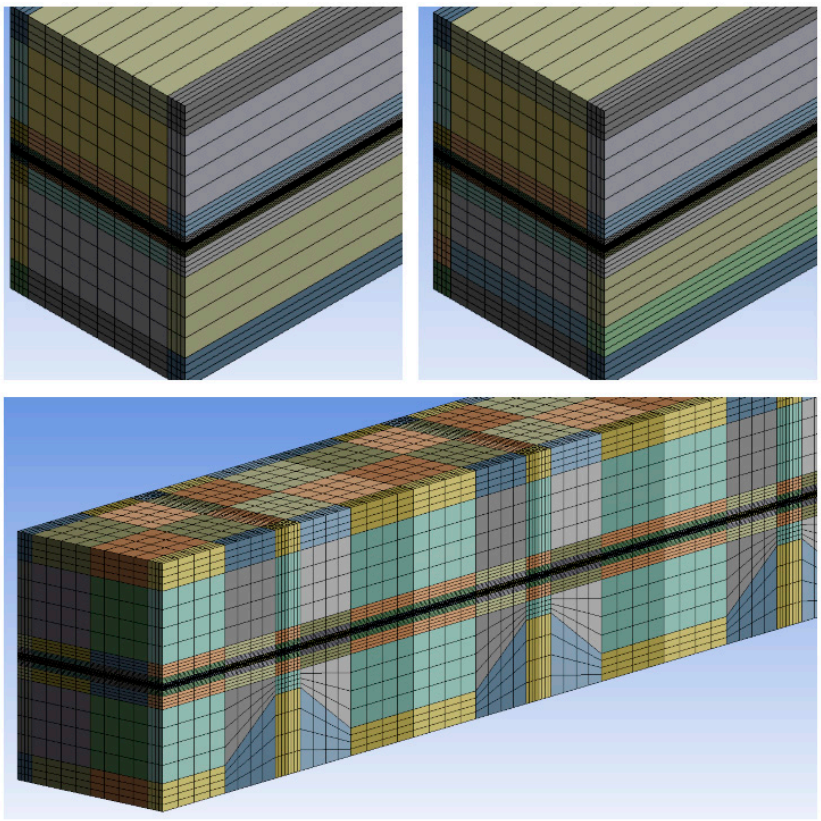

Figure S2. Mesh detail of conventional cathode channel and porous cathode channel geometry (above left); bi-porous cathode channel (above right); porous and baffled cathode channel (below).

As can be seen, the minimal number of subdivisions across the layers is 4. The porous and baffled channel mesh is very fine in the axial direction due to numerous restrictions in the channel cross-sections, while the axial discretization for conventional channel and bi-porous layer is 1 mm, which is sufficiently fine for this type of simulations, as seen in previous studies [22,28].

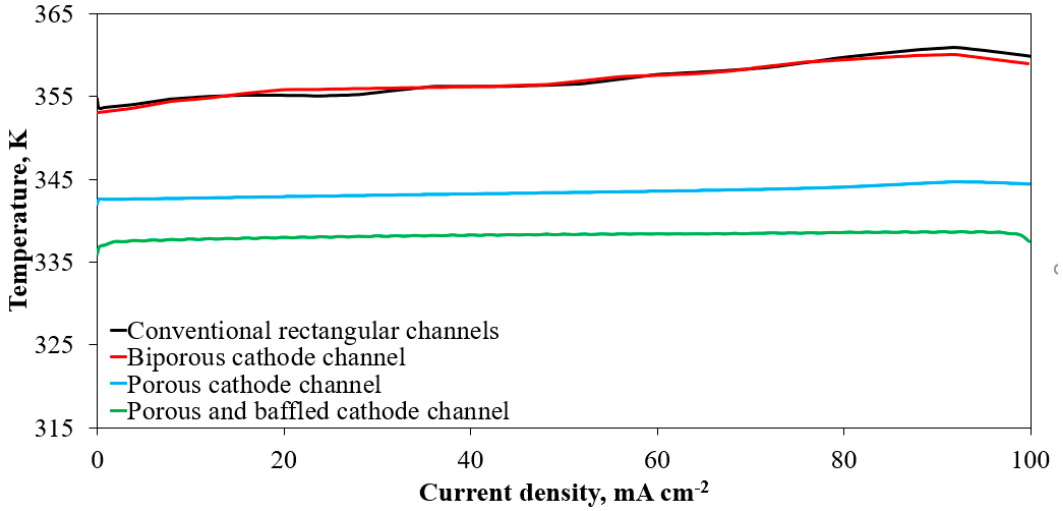

Figure S3. Temperature plots along the membrane mid-line at operating current density of 4.0 A cm^{-2}. The operating temperature is set to 328 K (i.e. 55 °C) at the current collector terminals,

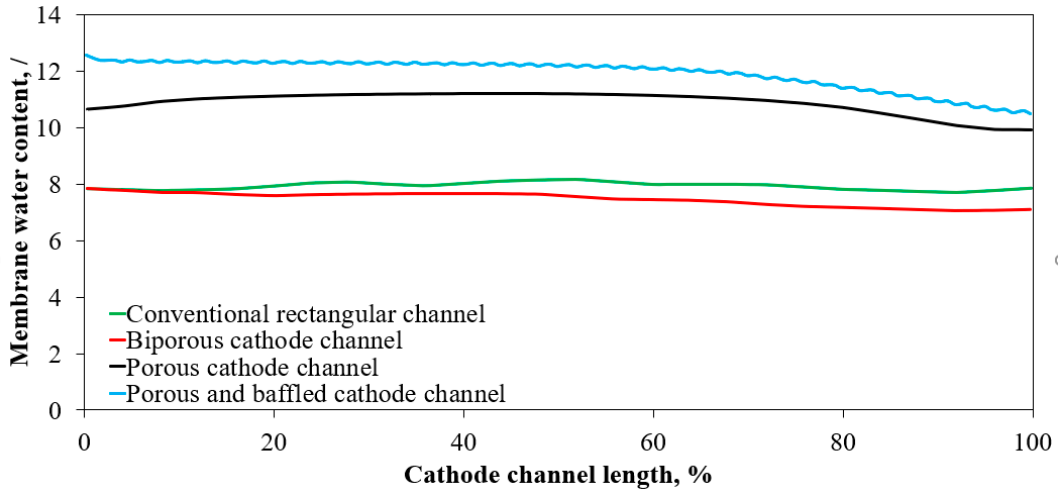

Figure S4. Membrane water content along the membrane mid-line at operating current density of 4.0 A cm^{-2}.

As a result of temperature built-up inside the MEA, the membrane water content is significantly lower for the conventional and bi-porous layer cases than that of the porous channel and porous and baffled channel, resulting in lower performance of the former two cases.

Table S1. Parameters and resulting electric potential at current density of 4.0 A cm^{-2} part 1/5.

Parameter (mm)	Ref. case	Case #1	Case #2	Case #3	Case #4	Case #5	Case #6	Case #7	Case #8	Case #9	Case #10
Half length segment	1	1	1	1	1	1	1	1	1	1	1
Half length baffle base	0.5	0.6	0.4	0.65	0.5	0.4	0.35	0.7	0.65	0.7	0.5
Half length baffle top	0.1	0.2	0.1	0.15	0.1	0.05	0.2	0.1	0.25	0.35	0.15
Thickness current collector cathode top	0.15	0.25	0.1	0.3	0.2	0.3	0.2	0.2	0.35	0.25	0.15
Height baffle	0.3	0.25	0.3	0.2	0.25	0.21	0.3	0.3	0.15	0.25	0.25
Distance baffle substrate	0.1	0.05	0.15	0.05	0.1	0.04	0.05	0.05	0.05	0.15	0.05
Electric potential (V):	0.51 5753	0.51 7451	0.51 1267	0.52 2654	0.51 8681	0.51 6568	0.52 2232	0.51 5933	0.51 9282	0.51 3656	0.51 6701

Table S2. Parameters and resulting electric potential at current density of 4.0 A cm^{-2} part 2/5.

Parameter (mm)	Case #11	Case #12	Case #13	Case #14	Case #15	Case #16	Case #17	Case #18	Case #19	Case #20	Case #21
Half length segment	1.2	1.2	1.2	1.2	1.2	1.2	1.2	1.2	1.2	1.2	0.8
Half length baffle base	0.65	0.35	0.65	0.4	0.5	0.6	0.4	0.7	0.45	0.6	0.5
Half length baffle top	0.15	0.2	0.25	0.1	0.1	0.15	0.15	0.25	0.05	0.25	0.1
Thickness current collector cathode top	0.3	0.2	0.35	0.1	0.15	0.2	0.25	0.2	0.25	0.25	0.15
Height baffle	0.2	0.3	0.15	0.35	0.3	0.35	0.35	0.3	0.35	0.4	0.3
Distance baffle substrate	0.05	0.05	0.05	0.05	0.1	0.1	0.1	0.1	0.1	0.15	0.1
Electric potential (V):	0.517 075	0.517 258	0.518 698	0.514 827	0.512 365	0.512 443	0.513 033	0.513 855	0.511 368	0.511 529	0.513 64

Table S3. Parameters and resulting electric potential at current density of 4.0 A cm^{-2} part 3/5.

Parameter (mm)	Case #22	Case #23	Case #24	Case #25	Case #26	Case #27	Case #28	Case #29	Case #30	Case #31	Case #32
Half length segment	0.8	0.8	0.8	0.8	0.8	0.8	0.8	0.8	1	1	1
Half length baffle base	0.55	0.45	0.55	0.55	0.55	0.4	0.35	0.45	0.55	0.45	0.5
Half length baffle top	0.05	0.15	0.05	0.2	0.1	0.15	0.05	0.15	0.05	0.15	0.1
Thickness current collector cathode top	0.15	0.15	0.2	0.2	0.15	0.1	0.1	0.25	0.1	0.1	0.1
Height baffle	0.2	0.2	0.45	0.35	0.25	0.2	0.15	0.35	0.2	0.2	0.15
Distance baffle substrate	0.1	0.1	0.1	0.05	0.05	0.05	0.05	0.05	0.025	0.025	0.025
Electric potential (V):	0.514259	0.515027	0.511903	0.517772	0.516938	0.517903	0.517304	0.516932	0.519137	0.520896	0.521184

Table S4. Parameters and resulting electric potential at current density of 4.0 A cm^{-2} part 4/5.

Parameter (mm)	Case #33	Case #34	Case #35	Case #36	Case #37	Case #38	Case #39	Case #40	Case #41	Case #42	Case #43
Half length segment	1	1	1	1	1.2	1.2	1.2	0.8	0.8	1	1
Half length baffle base	0.55	0.65	0.35	0.25	0.65	0.6	0.5	0.4	0.65	0.65	0.35
Half length baffle top	0.1	0.15	0.2	0.05	0.25	0.2	0.15	0.15	0.3	0.15	0.2
Thickness current collector cathode top	0.2	0.3	0.2	0.2	0.35	0.2	0.2	0.1	0.2	0.3	0.2
Height baffle	0.4	0.2	0.3	0.35	0.35	0.35	0.25	0.2	0.4	0.2	0.3
Distance baffle substrate	0.025	0.025	0.025	0.025	0.025	0.025	0.025	0.025	0.025	0.02	0.02
Electric potential (V):	0.517672	0.520807	0.521521	0.517017	0.521027	0.519921	0.519617	0.521716	0.524607	0.523019	0.51747

Table S5. Parameters and resulting electric potential at current density of 4.0 A cm^{-2} part 5/5.

Parameter (mm)	Case #44	Case #45	Case #46	Case #47	Case #48	Case #49
Half length segment	1	1	1.2	1.2	0.8	0.8
Half length baffle base	0.5	0.8	0.6	0.9	0.65	0.6
Half length baffle top	0.1	0.4	0.2	0.45	0.3	0.15
Thickness current collector cathode top	0.1	0.2	0.2	0.3	0.2	0.1
Height baffle	0.15	0.4	0.35	0.5	0.4	0.2
Distance baffle substrate	0.02	0.02	0.02	0.02	0.02	0.02
Electric potential (V):	0.522389	0.527433	0.521338	0.527106	0.526435	0.523954